Flexible Data and Frame Synchronization Structure for the LunaNet PNT Signal

Philip A Dafesh, Gourav K Khadge, Nathan S Wong and Goran Djuknic

The Aerospace Corporation

BIOGRAPHIES

Dr. Philip A. Dafesh is a Distinguished Engineer at the Aerospace Corporation specializing in GNSS signal design, signal processing, and applications of GNSS and software defied radio technology. He has contributed to the development of the modernized GPS signal structure and associated receiver processing for L1, L2C and M-code signals. Phil received B.S. degrees from California State Polytechnic University, Pomona in Electrical Engineering and Physics. He was granted M.S. and Ph.D. degrees in Electrical Engineering from UCLA. Dr. Dafesh has published 64 technical papers and was awarded 20 patents in GPS and related technologies with application to interference mitigation, constant envelope combining, signal design and receiver signal processing.

Mr. Gourav K. Khadge is a Member of Technical Staff in the Digital Communication Implementation Department of The Aerospace Corporation. He received his M.S. in Electrical Engineering in 2018 from the University of California, Los Angeles specializing in signals and systems. His current work is in research, analysis, testing, and development in wireless communications signals and systems, software defined radio, GPS and GNSS technologies. He has published two papers in IEEE and ION.

Mr. Nathan S. Wong is a Senior Member of Technical Staff in the Digital Communication Implementation Department of The Aerospace Corporation. He received his M.S. in Electrical Engineering in 2018 from the University of California, Los Angeles, with a research focus on information theory, error correction, and channel modeling. His current work and interests are software-defined radios and communication waveform design and validation. His previous work includes circuit design, machine learning, and system integration for aviation platforms.

Dr. Goran Djuknic is a Senior Communications Specialist at the Aerospace Corporation, specializing in wireless communications, signal processing, and GNSS signal design. His previous contributions to GNSS included interference mitigation algorithms, snapshot positioning, and GPS signal generation. At Raytheon Technologies, he developed innovative methods for wireless communication with sensors in airline cabins, cargo spaces, and outside and inside jet engines. He has also researched methods for modeling, simulation, and measurement of wireless propagation in confined spaces like airliners and elevator shafts. He has published 10 technical papers and has been awarded 14 patents.

ABSTRACT

A LunaNet Lunar Augmented Navigation Service (LANS) is being developed to enable a position, navigation, and timing service for future Lunar operations [1]. The signal includes two components. An in-phase data channel signal is spread by a 1.023 MCPS ranging code that provides a high-rate data message at 250 bps and is encoded by a strong Low Density Parity Check (LDPC) code. A pilot channel with a 5.115 MCPS spreading code is also provided. The pilot code is configured with a secondary (overlay) code that does not currently provide absolute time or frame Synchronization as is the case for L1C [2] [3]. This work shows the advantage of implementing an overlay structure that provides absolute time for the LunaNet LANS signal structure known as the Augmented Forward Signal (AFS).

The LunaNet AFS structure was developed to service two classes of user receivers. The first class is a low-complexity user receiver that only receives the 1.023 MCPS signal and does not use the 5.115 MCPS pilot channel. For this class of user, a data frame Sync word is needed. The second class of receiver is a high-end receiver that can process both data and pilot channels to take advantage of the higher chip rate pilot channel for enhanced robustness and improved accuracy. In the current draft LunaNet LANS AFS design, these users must employ the frame Sync word in the data channel and obtain absolute time after decoding the AFS navigation message [2]. The signal structure would greatly benefit from the addition of a pilot overlay structure that provides absolute time and robust frame Sync for high-end users as done for L1C [3]. To provide a more robust and interoperable AFS structure, this work summarizes a study and recommends alternatives for a new overlay code on the pilot channel that provides absolute time and a Sync word approach on the data channel.

The overlay code and Sync word are designed to allow for flexible and robust data synchronization for both low-complexity and high-end user receivers. The new overlay code structure permits frame synchronization performance that is as good as or better than the L1 C signal, while enabling a determination of absolute time upon frame Sync to aid high-end assisted LANS AFS user receivers at low signal to noise levels.

We also present the design of rate-matched 5G new radio (5GNR) LDPC codes that fit within the current 6000-symbol frame size along with a time of interval (TOI) word, frame ID (FID) word, and the remaining LunaNet AFS data message blocks. The paper describes and demonstrates robust frame Synchronization performance of the overlay code and Sync word approaches. The results are described in terms of probability of missed detection and probability of false alarm for a correct frame synchronization at low Eb/No levels expected for decoding the TOI word and LDPC encoded data. Advantages of the proposed data Synchronization structure will be described along with use cases for low-end and high-end receivers. Practical implementation considerations will also be described.

INTRODUCTION

LunaNet Position, Navigation and Timing (PNT) services are being specified to ensure an interoperable PNT broadcast service leverages developments and lessons learned from Earth-based global navigation satellite system (GNSS) to support a wide range of use cases, such as providing a precision navigation capability for the NASA Artemis missions. The draft signal specification defines two binary phase-shift keying (BPSK) signals: a 1.023 MCPS signal modulated with data and a 5.115 MCPS pilot signal modulated by an overlay code. The intent of the signal structure is to service both low complexity receivers that may only track the data channel, and high-performance receivers that will exploit all aspects of the signal including its higher chip rate pilot channel [1] [2].

The draft specification defines several aspects of the signal including the data and pilot channel spreading code rates. A number of these features, however, remained to be confirmed (TBC) [2]. These features include the data interleaving format, data and pilot overlay codes, spreading codes, the FID, TOI, final data message block sizes, and the specific LDPC coding. The specification is designed to be sufficiently flexible to accommodate different space (and potentially surface) based service providers with a unified common, flexible signal structure.

This work provides a trade study of signal aspects that are listed as TBC in the draft signal specification, including specific implementations of the features described above [2]. The paper will be organized as follows:

- Draft I and Q channel AFS Signal Design Description.
- I channel Signal Structure.
- Q channel Signal Structure.
- Summary and Conclusions.
- Acknowledgements.
- References.

DRAFT AFS I AND Q CHANNEL SIGNAL DESIGN DESCRIPTION

The draft LunaNet specification for AFS is depicted in Figure 1 [1][2]. The signal structure includes a data channel with LDPC coding like L1C, and with the provision to add features that are not present in L1C, including a

synchronization word for low complexity "lightweight" receivers wishing to only use the in-phase (I) data channel with its 1.023 MCPS ranging code. Details of the LDPC code, interleaving, ranging code period, FID, TOI and overlay codes are yet to be specified. Recommendations for the definition of these specific features will be described in subsequent sections based on the key design considerations and analyses.

The draft specification employs four subframes designated SB1, SB2, SB3 and SB4. SB1 includes the FID and TOI messages designed after the L1C signal structure. Each subframe employs 2 ms data symbols for a 500 MSym/sec rate. The FID allows flexibility to specify features of the AFS structure that have yet to be designed, such as different subframe designations.

The draft implementation allocates 104 symbols for the combination of sync word and SB1. Like L1C, SB2 contains the Clock and Ephemeris Data (CED) and is 1200 bits long that is a fixed time interval, while SB3 and SB4 contain variable data. SB2, SB3, and SB4 are rate ½ encoded. A subset of the data in SB2-4 is common to all providers, while some of the data may be provider specific. The SB2-4 data is interleaved to resist fading, while for SB1, we expect to use the same strong Bose–Chaudhuri–Hocquenghem (BCH) code used in L1C [3] [4] to enable decoding of TOI at C/N_0 levels well below L1C's LDPC code. Subsequent analysis will confirm this selection.

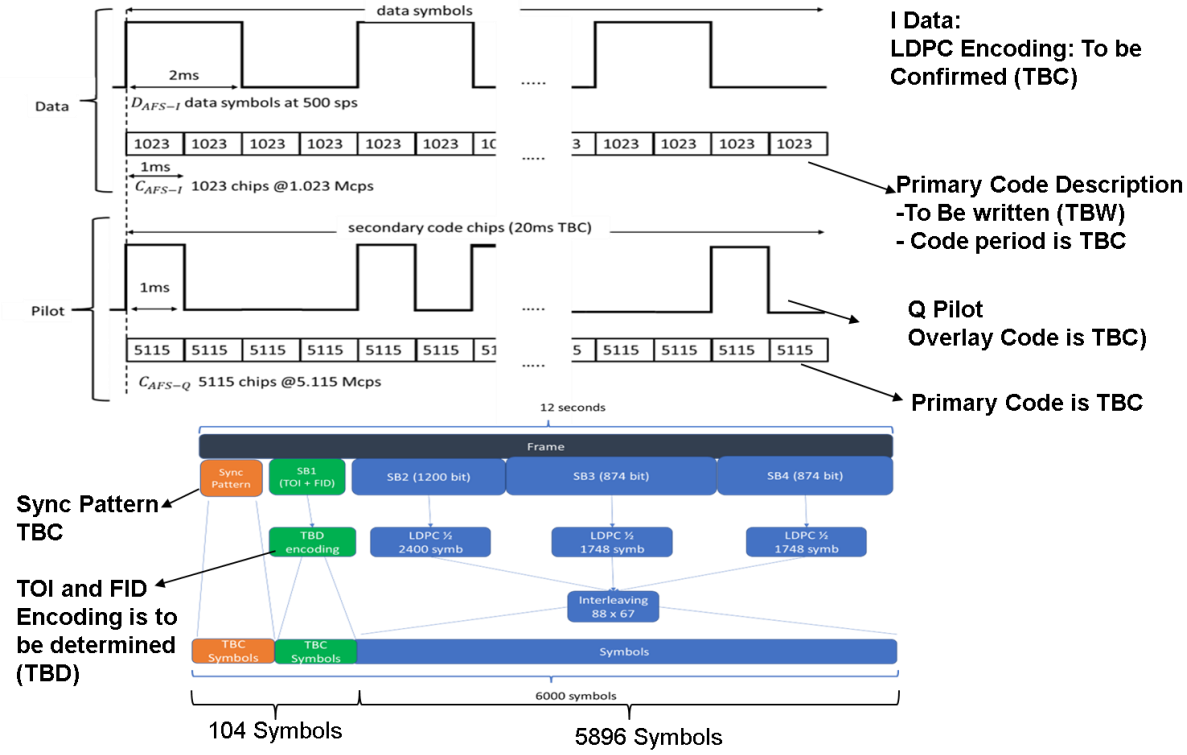

FIGURE 1: *Draft LunaNet augmented forward signal (AFS) structure [2].*

I CHANNEL SIGNAL STRUCTURE

1.1 I Channel Spreading Codes

Since the data symbol rate has been confirmed at 500 symbols per second, it is natural to select spreading code lengths that are aligned with the data symbol period of 2 ms, so that symbol synchronization can be achieved upon acquisition of the ranging codes. To achieve this, the I channel ranging code should be 2046 chips long, and the Q channel ranging code should be 10230 chips long. Extending the code period to the data symbol period is beneficial since it enables 2 ms coherent integration periods for the I channel.

A competing desire is reduced complexity of acquisition. One may assume that increasing the coherent integration period from 1 ms to 2 ms will increase receiver complexity by a factor of four (two-fold increase in the number of frequency cells to be searched and two-fold increase in the number of time cells), but this is not the case when comparing performance near the detection threshold, as described below. While an integration time of 2 ms increases the number of chips to search by a factor of two, it also reduces the amount of noncoherent integration that is needed to achieve a reliable signal acquisition [5] [6], and the increase in frequency search cells does not impact processing rate for a fixed Fast Fourier Transform (FFT) size [5] [6]. One must consider the fact that for over two decades Civilian Acquisition (C/A) code receivers have been capable of rapid parallel search over all 1023 C/A code chips (2046 time hypotheses for 1/2 chip spacing). Moreover, 32- and 64-point FFTs were the state of the art for conducting a parallel frequency search over 2 decades ago [9]. Thus, a 2046-chip sequence is appropriate for the I channel spreading code. Given advances in Moore's Law in over two decades, a 2046-chip data channel signal is well within the state of technology for low complexity receivers in the year 2020 and beyond [12]. This is evidenced by the development of modern ultra-low power receivers capable of acquiring the 1.023 MCPS C/A code, a 4092-chip binary offset carrier (BOC) modulated E1OS signal and a 2046-chip B1 signal at two to four times the complexity of a 2046-chip AFS I channel spreading code [13] [14].

Fifty 2046-chip Weil codes and fifty 2046-chip Gold codes were designed, and their auto and cross-correlation performance was compared to the 37 spreading codes of BeiDou's B1B signal, as well as the first 50 spreading codes for the GPS C/A code [7] [8]. Note that the Gold codes were designed by short cycling a 2047-chip Gold code [10], and the Weil sequences were designed according to the methodology in [11] by short cycling a 2053 length sequence. A comparison of the different I channel spreading codes is shown in **TABLE 1** below. The table illustrates the relative complexity of each option compared to C/A code and L5 code, as well as the code properties and cross-correlation performance with respect to rms, 99 %, 99.9 % and Max.

TABLE 1: Cross correlation results for 2046-chip AFS codes compared to C/A code and BeiDou's 2046-chip B1 code.

Code	1023 Chip C/A Code Acq.	1023 Chip C/A Code Track	Beidou B1 for AFS Acq./Track	New AFS 2046 chip Weil Acq/Track	New AFS 2046 chip Gold Acq/Track	AFS -Gold Max Cross Corr Improvement over CA	AFS - Gold Max Cross Corr Improvement over BeiDou
Coherent Integration (ms)	1	2	2	2	2	NA	NA
Code Length (Chips)	1023	1023	2046	2046	2046	NA	NA
Code Length (ms)	2	2	2	2	2	NA	NA
Code Rate (MCPS)	1.023	1.023	1.023	1.023	1.023	NA	NA
Acq. Complexity Relative to C/A	1	2	2	2	2	NA	NA
Acq. Complexity Relative to L5	0.01	0.01	0.02	0.02	0.02	NA	NA
RMS Cross-correlation (dB)	-30.1	-31.3	-33.1	-33.1	-33.1	3.0	0.0
99% Cross-correlation (dB)	-22.7	-23.9	-24.9	-24.9	-25.5	2.9	0.6
99.9% Cross-correlation (dB)	-20.8	-22.6	-22.8	-23.7	-23.7	2.8	0.9
Max (dB)	-20.3	-22.6	-22.8	-22.8	-23.7	3.4	0.9

The results show that the new Gold code provides up to a 3 dB performance improvement in acquisition and up to 2 dB in track compared to C/A Code with only a factor of two increase in search rate.

Overall, the new AFS Gold code has cross correlation performance that is up to 0.6 dB better than the 2046-chip Weil code and up to 1 dB better than BeiDou's B1 Gold code in the 99.9 % and 99 % confidence levels.

1.2 I Channel Data Synchronization Word

Unlike uncoded or convolutionally coded messages where reliable synchronization is not needed before decoding can begin, block coding schemes such as LDPC and BCH codes require frame synchronization before decoding can begin. Moreover, since the penalty for a frame synchronization error is large (at least 12 additional seconds – the duration of the data frame), this synchronization must be exceptionally reliable.

1.2.1 Theoretical Background and Methodology for Synchronization Word Design

As a basis for this analysis, it is assumed that the receiver has completed acquisition, as well as code and carrier lock. We will also assume that bit synchronization is automatically achieved when the code tracking loops have settled and that imperfections due to the code tracking loop precision on synchronization word detection can be ignored.

In this analysis, the receiver accumulates soft decision bits into a buffer for correlation against the synchronization word. Frame synchronization is achieved when the receiver computes a sequence of soft decision bits with sufficiently high correlation to the synchronization word, indicating the start of the frame. The decision threshold of the correlator must be chosen to sufficiently distinguish the correct synchronization word from noise. A decision threshold too high increases the risk of missing the detection of the synchronization word, and a decision threshold too low increases the risk of detection being triggered by noise leading to a false alarm.

Given a choice of synchronization word(s) consisting of L_S bits, the output of the correlator for a given sequence of received soft decision symbols, X, is as written below. Each soft decision symbol X_i is the sum of the value of the transmitted symbol B_i which is normalized to 1 or -1, and noise N_i which is normally distributed with a mean of zero and a standard deviation given by $\sqrt{\frac{R_b}{C/N_0}}$, where R_b is the bit rate in bits/sec of the signal and C/N_0 is the received carrier power to noise spectral density ratio in dBW-Hz after loss. For a correlation over L_s soft decisions X_i against the candidate overlay symbols S_i, we obtain

$$Corr(X) = \sum_{i=1}^{L_S} S_i X_i = \sum_{i=1}^{L_S} S_i(B_i + N_i) = \sum_{i=1}^{L_S} S_i B_i + \sum_{i=1}^{L_S} S_i N_i. \quad (1)$$

Where each soft decision contains a noise, N_i plus a signal component, B_i in volts.

The probability of missed detection is solely a function of the detection threshold, C/N_0 in the receiver, and the length of the synchronization word. When the received symbols in the buffer align with the synchronization word in the frame, $B_i = S_i$ and the first term reduces to L_S. The second term of the sum simplifies to a random variable following a normal distribution centered at zero with a standard deviation (in volts) given by:

$$\sigma_C = \sqrt{\frac{L_S * R_b}{C/N_0}}. \quad (2)$$

Thus, the correlator output is following a normal distribution as well, centered at L_S with a standard deviation given by σ_S. If the detection threshold in the receiver is given by V_T, then the probability of missed detection is given by applying the cumulative density function of the normal distribution expressed below. This calculation can also be inverted to choose a voltage threshold based on the desired probability of detection at a given C/N_0 as follows:

$$P_{MD} = \Phi\left(\frac{L_S - V_T}{\sigma_C}\right), \quad (3)$$

$$\mathrm{T} = L_S - \sigma_C \Phi^{-1}(P_{MD}), \quad (4)$$

where Φ is the cumulative density function of the normal distribution, and P_{MD} is the probability of a missed detection.

To analyze the rate of false alarms for a given choice of synchronization word, the sequence of bits in the frame outside of the synchronization word is assumed to be random and unbiased. It is also assumed that the incoming soft decision bits in the receiver start at a random and unbiased time relative to the start of the frame. Treating

each output of the correlator as a detection hypothesis, given a frame size of L_F bits, there is exactly one correct hypothesis in every sequence of L_F hypotheses. Thus, there are L_F-1 incorrect hypotheses per direct sequence of L_F hypotheses on which a false alarm can be triggered if the detection threshold is exceeded. The rate of false alarms is a function of the probability that an incorrect hypothesis will have a correlator output which exceeds the detection threshold. Of the L_F-1 incorrect hypotheses, there are 2*L_S-2 hypotheses in which the correlator output is a function of one or more bits from the true synchronization word. The remaining L_F-2*L_S+1 incorrect hypotheses have correlator outputs that are only functions of bits not in the synchronization word. To simplify the analysis, the term in the correlation equation below is simplified to separate the summation for the elements in the received symbol buffer which are part of the synchronization word and a second summation for the elements in the received symbol buffer which are not part of the synchronization word. This may be expressed by:

$$\sum_{i=1}^{L_S} S_i B_i = \sum_{i \in S} P_{MD} S_i B_i + \sum_{i \notin S} S_i B_i. \quad (5)$$

For each hypothesis, the first term is fixed and easily calculated, while the second term is a randomly distributed variable. Letting **J** be the number of symbols in the buffer not in the synchronization word, and **K** be the number of symbols in the summation for which $S_i \neq B_i$, the second term can be further simplified as follows:

$$\sum_{i \notin S} S_i B_i = J - 2K, \quad (6)$$

$$Corr(X) = \sum_{i \epsilon S} S_i B_i + (J - 2K) + \sum_{i=1}^{L_S} S_i N_i, \quad (7)$$

Notably, K is a discrete random variable which follows a binomial distribution with n=J and p=0.5. For any value k in the distribution of K, Corr(X) becomes a normal distribution with mean $(\sum_{i \epsilon S} S_i B_i) + (J - 2k)$ and with a standard deviation of σ_S. Thus,

$$P_{FA|H,k} = \Phi\left(\frac{(\sum_{i \epsilon S} S_i B_i) + (J - 2k) - T}{\sigma_C}\right). \quad (8)$$

We can then take the expected value of $P_{FA|H,k}$ over all possible k, giving us the probability of false alarm (FA) for a given hypothesis as follows:

$$P_{FA|H} = \sum_{k=0}^{J} \binom{J}{k} 0.5^J \Phi\left(\frac{(\sum_{i \epsilon S} S_i B_i) + (J - 2k) - T}{\sigma_C}\right). \quad (9)$$

This expression is then used to calculate the false alarm rate as the expected number of false alarms per frame. The expected number of false alarms per frame is the summation of the expected number of false alarms per hypothesis, summed over all hypotheses. For the hypothesis that is correct, the expected number of false alarms is zero, since a trigger of the detection threshold would result in correct detection, not a false alarm. For every other hypothesis, one false alarm is contributed with probability $P_{FA|H}$, and zero false alarms are contributed with probability $1 - P_{fa|H}$. Thus, the expected number of false alarms contributed by each of these hypotheses is $P_{fa|H}$. Letting H_C represent the hypothesis that is correct is given by:

$$E[fa] = \sum_{H \neq H_C} P_{fa|H}. \quad (10)$$

This also allows us to calculate the expected number of false alarms per hypothesis, which is just this number divided by the number of possible hypotheses that could result in a false alarm, i.e.,

$$False\ Alarms\ per\ Hypothesis = \frac{E[FA]}{L_S - 1}. \quad (11)$$

1.2.2 Data Frame Synchronization Performance of C/A and E10S

C/A code and E1OS have uncoded 8- and 10-bit synchronization words every 6 sec and every 1 sec, respectively, allowing flexibility to achieve any desired reliability before declaring a frame synchronization. For example, a detection can be declared after acquiring 1 of 1 synchronization words, 2 of 2 synchronization words, 3 of 3 synchronization words, etc., depending on the desired reliability. Furthermore, since the synchronization words appear several times within a data message, the time to verify a false alarm can be quite small making it acceptable to operate at higher false alarm rates.

TABLE 2 and **TABLE 3** show synchronization performance and probability of detection results for C/A code and E1OS, respectively. For each case, the C/N_0, was set and the detection threshold was adjusted until the desired probability of detection, P_d, was met. A Monte Carlo simulation was then run until the false alarm probability, P_{fa}, sufficiently converged (usually after at least 100 false alarms were detected).

TABLE 2: Synchronization performance for 1 of 1, 2 of 2, and 3 of 3 synchronization detection strategies vs probability of detection for C/A code.

C/A Code Sync Word Performance at C/No =28 dB-Hz	**Pd = 0.90**			**Pd=.95**			**Pd=.99**		
	1 of 1	2 of 2	3 of 3	1 of 1	2 of 2	3 of 3	1 of 1	2 of 2	3 of 3
False alarms per 300 symbol frame	1.1200	0.0061	0.0000	1.3270	0.0090	0.0001	2.1100	0.0238	0.0003
Pfa per Hypothesis	3.75E-03	2.04E-05	1.37E-07	4.44E-03	3.01E-05	2.31E-07	7.06E-03	7.96E-05	1.04E-06
Max Time to frame Sync (sec)	12	18	24	12	18	24	12	18	24
Max time to read CED (sec)	30	30	30	30	30	30	30	30	30

TABLE 3: Synchronization performance for 1 of 1, 2 of 2 and 3 of 3 synchronization detection strategies vs probability of detection for the E1B data signal of E1OS.

E1B Code Sync Word Performance at C/No =28 dB-Hz	**Pd = 0.90**			**Pd=.95**			**Pd=.99**		
	1 of 1	2 of 2	3 of 3	1 of 1	2 of 2	3 of 3	1 of 1	2 of 2	3 of 3
False alarms per 250 symbol frame	2.6600	0.0695	0.0023	4.1500	0.1460	0.0063	8.7976	0.5268	0.0368
Pfa per Hypothesis	1.07E-02	2.79E-04	9.24E-06	1.67E-02	5.86E-04	2.53E-05	3.53E-02	2.12E-03	1.48E-04
Max Time to frame Sync (sec)	12	18	24	12	18	24	12	18	24
Max time to read CED (sec)	30	30	30	30	30	30	30	30	30

As observed, the number of false alarms per message can be less than 0.04 with a detection probability of, $P_d = 0.99$. and less than 0.001 with, $P_d = 0.95$. A 95 % confidence is required for avionic applications and guarantees a sufficient level of reliability for comparing data message performance [15] [16]. A 95 % Time To First Fix (TTFF) requires that acquisition of four satellites and frame synchronization be achieved with a 99 % confidence since $0.99^5 \approx 95\ \%$. Thus, with 99 % detection probability, and a 6000-symbol AFS frame, it is desirable to have less than one false alarm in 100 or more frames, or $6000 \times P_{fa} \ll .01$. Thus, a minimum acceptable false alarm rate of 1E-06 is appropriate for the AFS synchronization word. Note that since all soft decisions in a 30 second frame can be saved in memory, frame synchronization and message decoding can be performed once 30 seconds worth

of soft decisions are recorded. There is no need for these operations to be conducted sequentially in wall clock time.

Unlike high reliability frame synchronizing using an overlay code as in L1C, high reliability frame synchronization using the data channel alone (or low size weight and power (SWAP) receivers) can only be achieved by acquiring a Sync word with sufficiently low P_d and P_{fa} at the minimum C/N_0 level expected for the data encoding. In the next section, we will describe the design and simulation of the LunaNet AFS data channel synchronization word and compare performance vs length in symbols and the duration in time.

1.2.3 Design of the LunaNet I Channel Data Frame Synchronization Word

Synchronization words of various lengths were analyzed for their rate of false alarms per hypothesis. Each synchronization word was chosen from sequences with minimum peak sidelobe levels after autocorrelation. Selecting synchronization words with high peak autocorrelation sidelobes caused notable increases in the false alarm rate. Synchronization words of lengths 52, 64, 68, and 128 were analyzed. The plot of false alarm rate per hypothesis vs C/N_0 for a 68-symbol synchronization word is shown FIGURE 2 below. The codes were selected from reference [17].

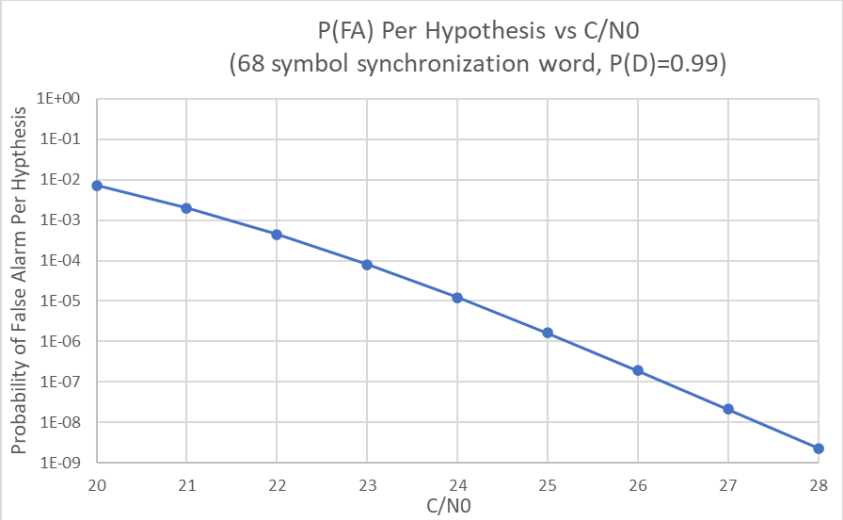

FIGURE 2: False alarm probability vs C/N_0 for a 68-symbol synchronization word.

For each of these synchronization words, we found the minimum C/N_0 such that the false alarm rate per hypothesis was below 1E-06. The minimum C/N_0 for each synchronization word to achieve the desired performance is shown in TABLE 4.

TABLE 4: Synchronization Word Performance vs Length

Sync Word Length (Symbols)	Sync Word Length (ms)	Minimum C/N_0 (dB-Hz)
52	104	27.41
64	128	25.69
68	136	25.23
128	256	21.16

The synchronization word design was conducted in parallel with forward error control design to ensure that a single synchronization word could operate down to the level of the BCH code and CED C/N_0 threshold levels, while still permitting reasonable factoring of the data blocks for subsequent interleaving. Considering that the I channel may be useful for low complexity user receivers which may not require operation to this level, a 68-bit

synchronization word was identified as having more than adequate performance, and operates below the threshold for CED data demodulation to be described in the following section.

1.3 Forward Error Control Coding

1.3.1 SB1 Data Encoding

The draft version of the AFS specification allocates 104 symbols for sync word and SB1. SB1 can be assumed to be composed of 52-symbol messages. In this work, we will examine the performance of SB1 encoding assuming it is based on L1C's rate 9/52 BCH code [3]. As will be shown in 1.3.2 below, and described in [3], the rate 9/52 L1C BCH code enables operation to a minimum E_b/N_0 threshold of 5.61 dB for a bit error rate (BER) of 1E-05 or 2.71 for a message error rate (MER) of 1E-01. This corresponds to $C/N_0 = 5.61 + 10Log(500 \times 9/52) = 25\ dB - Hz$ for the BER threshold and 22 dB-Hz for the MER threshold. As with L1C, the LDPC encoding is expected to require a higher minimum C/N_0 threshold for reliable operation. One purpose of the TOI is to permit code combining [3] (more appropriately named CED combining) where soft decisions of successive frames of CED data are coherently combined to permit lower data thresholds (e.g., 3 dB lower for two frames). This approach is illustrated by **FIGURE 3**. In the figure, the orange highlighted numbers represent soft decisions that are coherently combined to enable decoding of the message at lower C/N_0 levels. This is not the case for the FID, however, which is designed to provide flexibility for future options to the AFS subframe structure or provider information [1] [2]. While L1C requires that the TOI be equal to the message update period, this approach is not needed to perform CED combining of message soft decisions since one only needs to know when the CED message changes. To provide flexibility to change the overall data frame structure (e.g., interleaving different portions of the message), 2 bits of the BCH codes can be used to provide FID, while the remaining 7 can be used to define an interval of time up to 20 minutes wherein the CED data doesn't change. The Time of Week (TOW) would thus be made up of 7 bits and 9 additional bits in the interval time of week within the CED message (SB2).

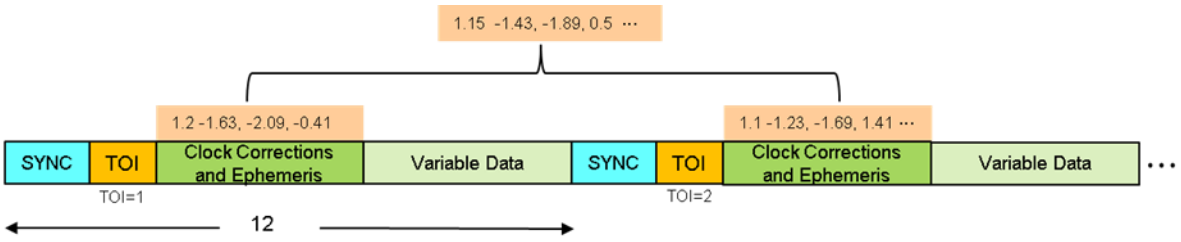

FIGURE 3: Illustration of CED combining.

1.3.2 LDPC Forward Error Control Coding

The proposed forward error correction (FEC) scheme for SB2, SB3, and SB4 (and combinations thereof) is a flavor of the 5G NR-LDPC code design [18]. The 5G NR-LDPC codes are rate-compatible, protograph-based solutions that allow for flexibility when designing a frame size [19]. These codes were chosen to enable flexibility in the LunaNet AFS design and ease of implementation due to broadly available intellectual property (IP).

The LunaNet AFS frame sizes and rates are within reasonable bounds for what is recommended for use with the 5G 3rd Generation Partnership Project (3GPP)'s FEC approach. As described above in Section 1.2, a trade study was conducted with different frame sizes based on synchronization word requirements for the I channel. The frame structure in **FIGURE 4** below depicts a baseline recommendation and was used to design the LDPC codes based on the 5G NR methodology. In addition, a trade study was conducted to determine the pros and cons of combining SB3 and SB4 into a larger data block (resulting in an SB2+SB3 subframe set). The combination of SB2 into one large block (SB2+SB3+SB4) was also considered, but is not recommended since it would negate the functional utility of

having the TOI in SB1 to do code combining.

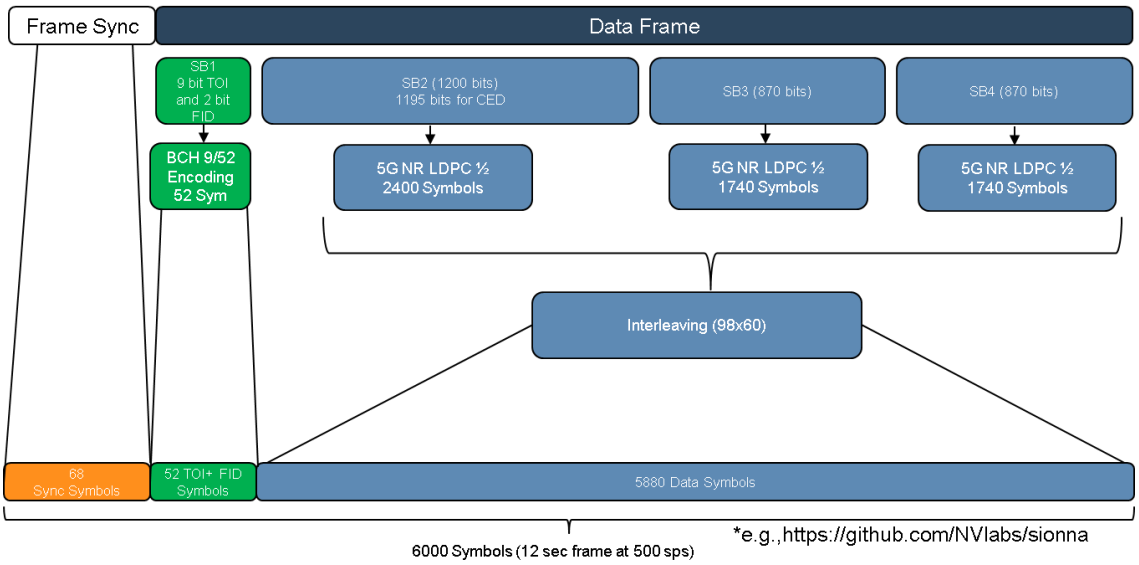

FIGURE 4: Baseline Frame structure.

The design process was derived from the technical specification for 5G NR multiplexing and channel coding (3GPP Technical Specification 38.212) and validated via open-source libraries [20]. Usage of such a flexible family of codes allows for a unified design approach that can be applied to future frame design choices aside from the default, denoted by FID =0. For this comparison, the FEC error rate plots were simulated using an application de-mapping method, box-plus check node calculation, and 20 decoding iterations [20]. Theoretical LDPC decoding calculations normally rely on standard belief propagation for check node calculations but are not practical due to their complexity [21]. The box-plus algorithm was used for check node calculations.

Each error correction code was simulated in an Additive White Gaussian Noise (AWGN) environment with a Monte Carlo process and independent noise samples. Data is collected for every C/N_0 point until a minimum of 100 errors is reached. The Monte Carlo technique is applied by first creating a random message then encoding it using the appropriate FEC. In the case of CED combining, the random message is identical for the combined pair, but the noise samples are independent of each other. Log Likelihood Ratios (LLRs) calculated in the decoding process assume a priori knowledge of the noise samples. For CED combining, the two codewords are summed after the LLR calculation stage.

The results shown in **FIGURE 5** below illustrate the performance of the AFS options as compared to TOI, L1C, E1OS, L5, E5 and C/A code in terms of BER. The LunaNet 5G NR FEC alternatives far outperform the message performance (in terms of E_b/N_0) of all satellite navigation systems. In particular, the AFS FEC can demodulate CED data at 0.6 dB lower E_b/N_0 than L1C, 2.8 dB lower E_b/N_0 than E1OS or L5, and 7.9 dB lower E_b/N_0than C/A code to achieve the same BER. Figure 6 also shows the performance in terms of $\frac{C}{N_0}$, which will vary due to the different data rates of each signal.

Note that while the BER of the TOI/FID BCH code performs worse in terms of E_b/N_0, its performance vs C/N_0 is more than 3 dB lower than the LDPC code, especially at the MER threshold of 1E-02 as observed by **FIGURE 7**.

This enables the TOI to be used to determine whether the next CED frame has changed or not. If it has not, then soft decisions can be combined using CED combining. **FIGURE 7** illustrates simulation results of this approach showing that the full 3 dB performance improvement may be achieved by combining soft decisions from successive frames.

To our knowledge, this is the first simulation of CED combining. The results illustrate that CED can be decoded at C/N_0 levels as low as 22.5 dB to achieve a message error rate of 1E-02 and data read time of 24 seconds. Thus, data demodulation sensitivity can be traded against time to decode data.

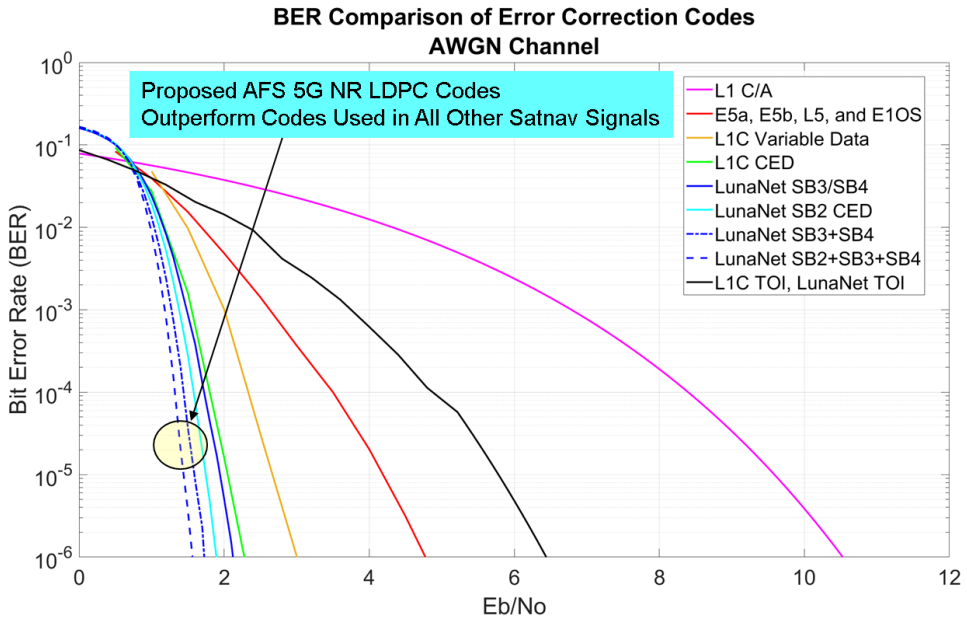

FIGURE 5: Comparison of LunaNet AFS FEC alternatives under consideration in terms of BER vs E_b/N_0.

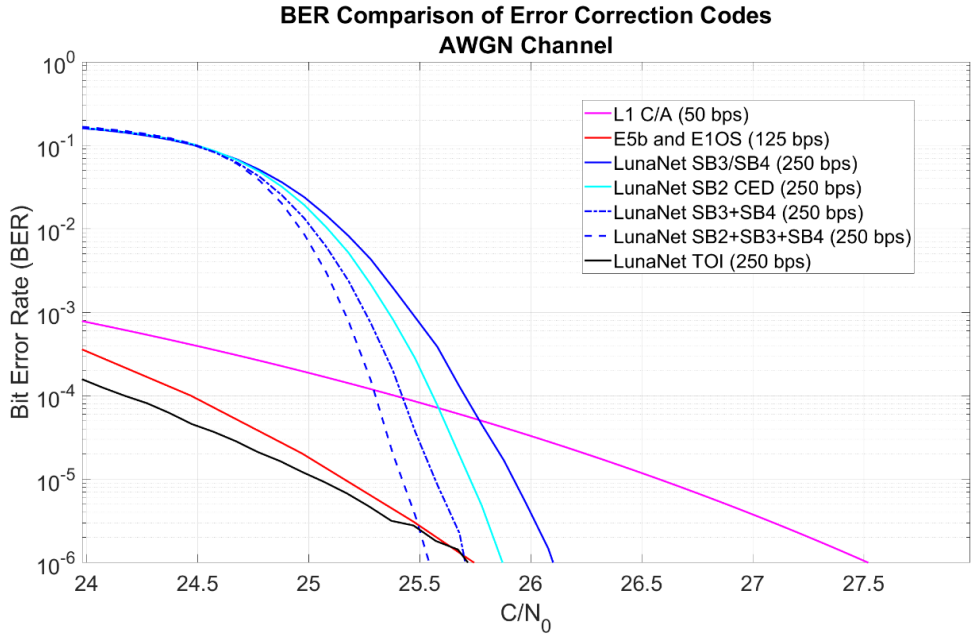

FIGURE 6: Comparison of Lunanet AFS FEC alternatives in terms of BER vs C/N_0.

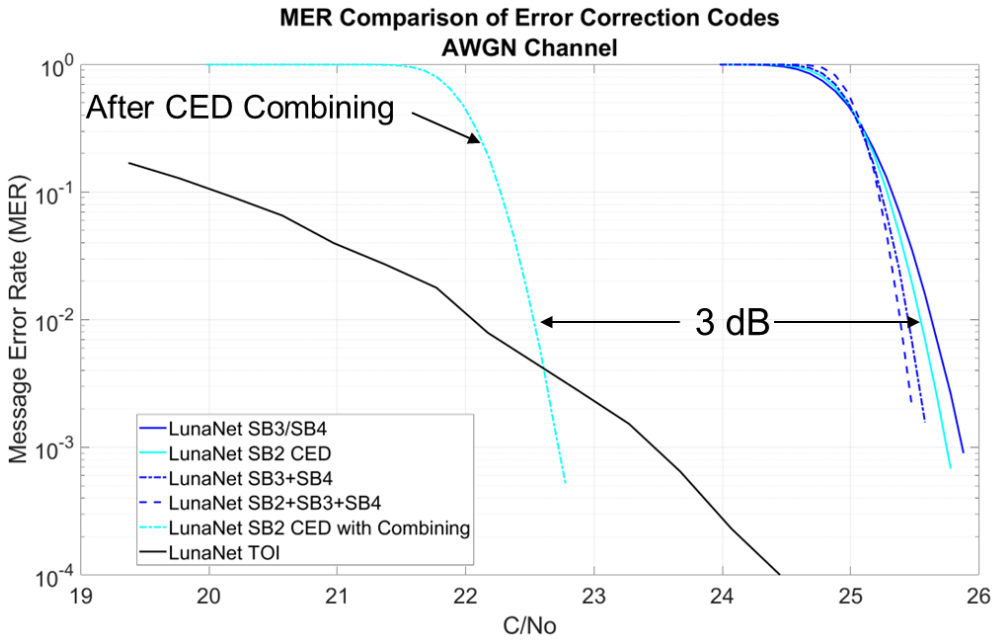

FIGURE 7: Illustration of CED combining to improve LunaNet AFS BER by 3 dB.

Q CHANNEL SIGNAL STRUCTURE

1.4 Spreading and Overlay Codes

To serve the needs of high-end users, it is desirable for the LunaNet AFS to also enable frame synchronization using the pilot channel in a method analogous to the L1C signal. The current draft signal structure did not address absolute time with the pilot signal because of the repeating nature of the overlay code. Thus, to achieve high reliability frame synchronization using the pilot channel, an overlay code scheme is needed that provides a receiver with time to one primary code chip.

This can be achieved using a single secondary overlay code with 6000 chips (3.33 times the length of L1C). A more flexible alternative is to employ repeating secondary and tertiary overlay codes to provide improved acquisition flexibility and robustness, by enabling a receiver to acquire on one of two different pilot channel spreading codes or the 2046 chip data channel spreading code. An example of this approach is shown in **FIGURE 8**. The tertiary overlay approach enables greater receiver design options and reduces the length of the outer overlay code, enabling a lower complexity search to achieve absolute time synchronization.

In this option, a 10230-chip, 2 ms primary code was selected along with four orthogonal 4-chip overlay codes: 1110, 1101, 1011, and 0111 that are randomly distributed to different satellites within the constellation such that the statistics of the cross-correlation performance are improved. The sequence 1110 was used from the E5b-I [14] and the remainder are circular shifts of this sequence that have similar auto- and cross-correlation properties yet are orthogonal to each other.

For purposes of analysis, fifty 1500-symbol tertiary overlay codes were designed from a 1499-chip Weil sequence that was padded by one chip using the methodology described in [11]. The 10230-chip E5b code was used as the primary code for comparative analysis. An alternative primary code may be selected in the final design of LunaNet AFS, such as the L5 or L1C code families, which both have 210 codes defined, or a newly designed code.

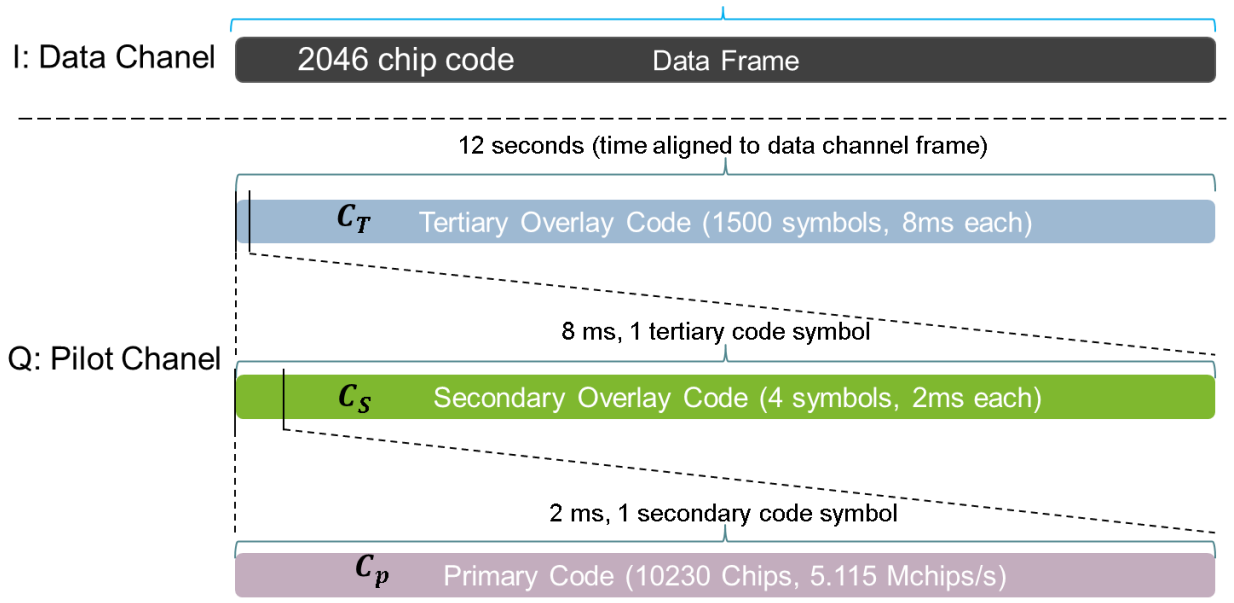

FIGURE 8: Tiered overlay approach with primary, secondary, and potentially tertiary overlay codes.

To our knowledge, this work describes the first application of tertiary overlay codes in satellite navigation systems and provides unique opportunities for use cases that trade acquisition complexity with performance. This is especially useful in navigation systems that employ data rates that are higher than legacy 50 bits/sec rates, as specified for AFS. Without the tertiary code, a receiver without accurate time cannot acquire with integration periods beyond 2 ms. By introducing a short secondary code and a longer tertiary code, a high-end receiver with an acquisition capability comparable to L5-only receivers, can acquire the repeating 8 ms code without first acquiring the I channel code to enable acquisition with more than 10 dB of added processing gain [23]. This is compared to acquisition of the 2046-chip I channel spreading code. The complexity of acquiring the tiered 8 ms overlay and primary code is only two times greater than L5 since the complexity scales with the code length, code rate, and AFS pilot code rate is one-half that of L5.

Overall, five pilot options were studied, as identified in Table 5. For each option, the best 50 outer codes (tertiary for Options 1-4 and secondary for Option 5) were designed from Weil or Gold sequences with good autocorrelation and cross-correlation properties. The reader is referred to [11] and [24] for explanation of how to determine sequences with good correlation properties, as this determination is beyond the scope of the present paper.

The configuration of each option in terms of primary, secondary, and tertiary is described in **TABLE 5**. Option 1 mirrors the E6 signal with a 5115-chip E6C primary code and 100-chip E6 secondary code, but adds a 120-symbol tertiary code that was designed from a of short cycled 127-chip Gold code [10] [22]. This choice allows a receiver to obtain absolute time to a resolution of one primary code chip once the tertiary code is synchronized.

Option 2 employs the E5b-I primary code along with the 100-symbol E6C overlay code and fifty 60-symbol tertiary code sequences constructed from a short cycled 63-chip Gold code sequence[10] [22]. Again, the tertiary sequence provides absolute time.

Option 3 was described above in **FIGURE 8**. Option 4 also uses the 10230-chip E5B sequence and a set of 24 orthogonal 10-bit Neuman-Hoffman sequences with good auto- and cross-correlation properties that were randomly assigned to 50 primary codes to improve overall correlation statistics. For this option, a family of 50 Weil

code sequences was designed by short cycling a length-601 Weil sequence, as described above for the other code designs.

Finally, option 5 uses a 10230-chip E5B primary code along with a family of 50 secondary outer overlay codes that were designed from a length-6007 Weil code sequence that was short cycled to 6000 symbols.

TABLE 5: Pilot channel options with primary, secondary, and tertiary codes.

Option	Primary Symbols	Secondary Symbols	Tertiary Symbols	Outer Code	Primary Code Used for Simulation
1	5115	100	120	Tertiary	E6C
2	10230	100	60	Tertiary	E5B
3	10230	4	1500	Tertiary	E5B
4	10230	10	600	Tertiary	E5B
5	10230	6000	N/A	Secondary	E5B

1.5 Overlay Code Design and Simulation

For each configuration, only the number of symbols in the highest-level overlay codes were relevant for analysis of synchronization performance. Thus, five overlay codes were analyzed having length 120, 60, 1500, 600, and 6000. These alternatives correspond to Options 1-5 in **TABLE 5** above.

As in the synchronization word analysis, the signal receiver produces soft decisions after synchronizing commences with the primary code (option 5) or the tiered product of primary and secondary codes (Options 1-4). In Options 1-2, this synchronization must be achieved by performing a secondary search over 50 possible offsets of the primary code with the secondary code. This can be achieved in a very robust manner by coherently accumulating several soft decisions for each trial required to achieve a given sensitivity that is well below the level of the BCH decoder.

For Option 3, it is feasible for a receiver to achieve synchronization with the secondary code by directly acquiring the 10230x4 = 40920-chip tiered code or searching over 4 possible offsets with the secondary code, which can be performed very reliably in under 0.5 sec.

After this step, absolute time is obtained by feeding some number of soft decision outputs from the correlator (integrating over the period of the outer code symbols) into a buffer memory, and the received sequence is correlated against all possible positions in the frame. For an overlay code of length L_0, there are L_0 hypotheses for the position of the received sequence in the frame. This is true since after code and carrier tracking, the search can be conducted in 1-chip increments, entirely in software, without chip quantization or frequency scalloping loss.

Two synchronization strategies were considered in this analysis. In one strategy, a threshold is applied and the first hypothesis which exceeds that threshold is considered as the chosen hypothesis. In the second strategy, all hypotheses are tested and the hypothesis with the maximum correlation to the received sequence is considered as the chosen hypothesis. That is, treating the sequence as an information symbol that provides absolute time via maximum likelihood decoding.

The performance of both strategies is a function of the amount of time (number of soft decisions) the receiver takes before deciding the correctly hypothesized overlay timing, as well as the received C/N_0. For this analysis, let L_R be the number of symbols accumulated by the receiver. For this analysis, a Monte Carlo algorithm was employed to estimate the performance.

For each Monte Carlo trial, a position in the overlay code was chosen at random. L_R symbols from this position were loaded into a buffer and white Gaussian noise was added to each symbol to represent noisy soft decision symbols. The buffer was then correlated against all possible positions in the overlay code, giving L_O hypotheses. The output of the correlation buffer at a given position is shown below.

$$Corr(X) = \sum_{i=1}^{L_R} O_i X_i = \sum_{i=1}^{L_R} O_i (B_i + N_i) = \sum_{i=1}^{L_R} O_i B_i + \sum_{i=1}^{L_R} O_i N_i. \quad (12)$$

For the hypothesis that is correct, the output of the correlator will be a random variable normally distributed with a mean of L_R and a standard deviation given by $\sigma_C = \sqrt{\frac{L_r * r}{C/N_0}}$ where r is the symbol rate of the overlay code. Thus, given a threshold T, probability of missed detection can be calculated as below,

$$P_{MD} = \Phi\left(\frac{L_R - T}{\sigma_C}\right), \quad (13)$$

And a threshold for a desired probability of missed detection level for a given C/N_0 can thus be derived from

$$\mathrm{T} = L_R - \sigma_C \Phi^{-1}(P_{MD}). \quad (14)$$

For each Monte Carlo trial, the number of failed detections of the correct hypothesis and the number of false hypotheses that trigger the detection threshold are recorded and added to a running total. The missed detection rate is estimated by dividing the accumulated number of failed detections by the number of trials. The expected number of false alarms is similarly estimated by dividing the accumulated number of false alarms by the number of trials. Additionally, for the maximum likelihood strategy, the Monte Carlo algorithm accumulates the number of trials in which the maximum likelihood strategy identifies the correct hypothesis. The number of successes divided by the number of trials gives the estimated success rate of this strategy. The Monte Carlo algorithm is run until sufficient convergence is reached.

1.6 Overlay Code Time to Synchronization Performance

Results of the threshold strategy for the 1500-symbol overlay over various dwell times are shown below for the case of a C/N_0 of 25.2 dB-Hz. The expected rate of false alarms was below 1E-05 (per hypothesis or per frame) in under 0.8 seconds as shown in **FIGURE 9**. Using a maximum likelihood estimation approach, a probability of error below 1E-06 is achieved in under 0.5 seconds as illustrated by **FIGURE 10**.

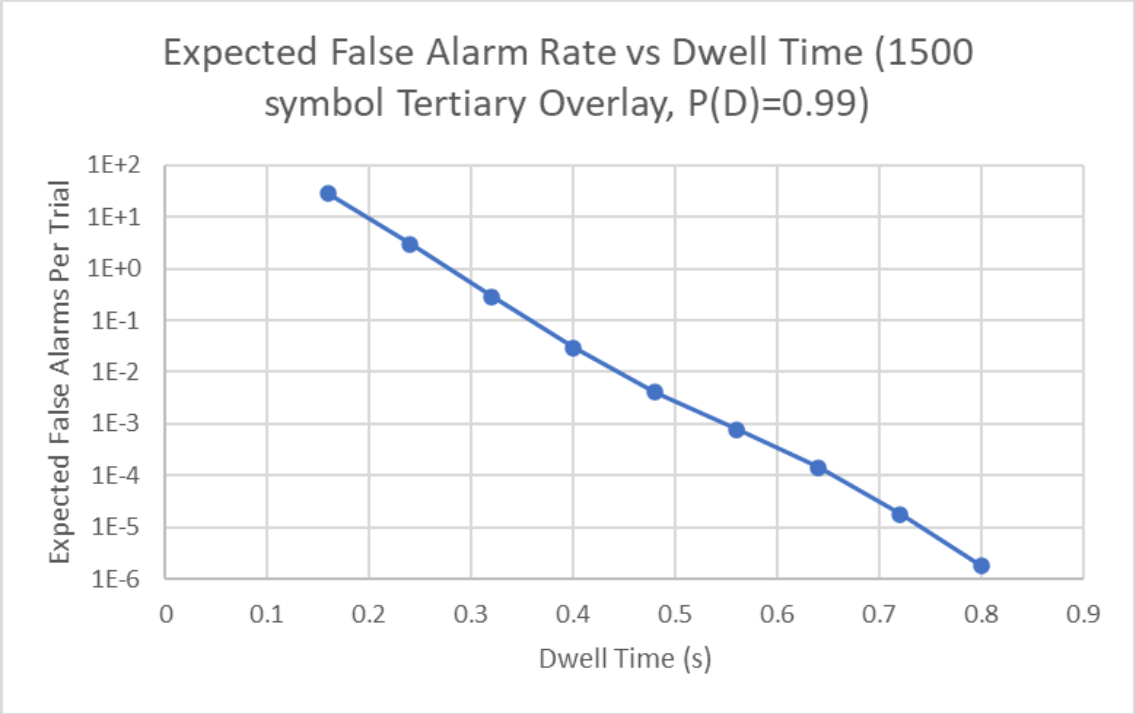

FIGURE 9: False alarm rate per trial for threshold synchronization method.

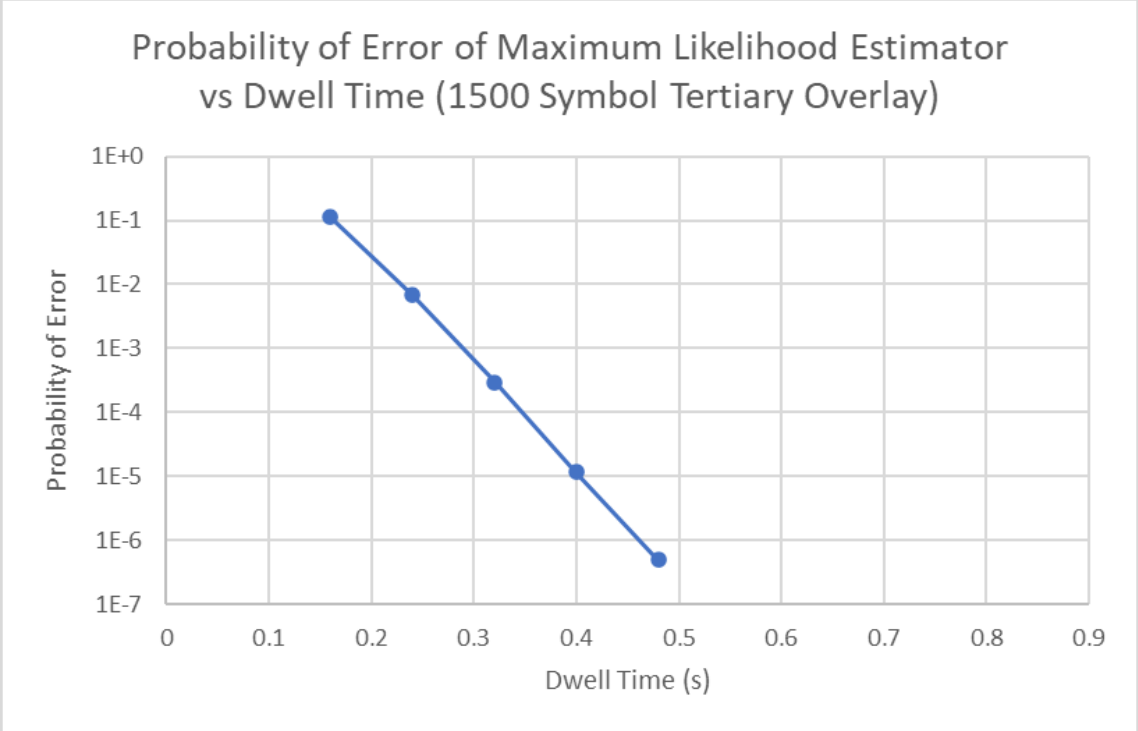

FIGURE 10: Probability of synchronization error vs dwell time for maximum liklihood detection approach.

In both approaches, synchronization performance improves with increased dwell time (number symbols integrated), but the maximum likelihood detection approach simplifies the search in that it does not require a

detection threshold and tends to achieve overall lower time to synchronize. As a result, the maximum likelihood estimator was used to compare the synchronization time of each option as shown in Note that the time includes the dwell time plus 100 ms to collect the required soft decisions plus 100 ms to search over all possible overlay code offsets.

TABLE 6 below. Note that the time includes the dwell time plus 100 ms to collect the required soft decisions plus 100 ms to search over all possible overlay code offsets.

TABLE 6: Time to synchronize overlay sequence with a maximum likelihood estimator.

Option	Primary Symbols	Secondary Symbols	Tertiary Symbols	Outer Code	Primary Code Used for Simulation	Time to Sync (Sec)
1	5115	100	120	Tertiary	E6C	1.7
2	10230	100	60	Tertiary	E5B	2.7
3	10230	4	1500	Tertiary	E5B	0.284
4	10230	10	600	Tertiary	E5B	0.46
5	10230	6000	N/A	Secondary	E5B	0.176

Notice that the time to synchronize with Option 5 requires the least time due to better correlation properties of the longer overlay code. Even for Option 5, which required the greatest number of search hypotheses, the elapsed time to synchronize the code took less than 10 ms using a desktop PC running Python. Option 3 provides the 2nd longest tertiary code, resulting in good correlation properties as confirmed with a 2nd lowest time to synchronize amongst options. Overall, option 3 has an attractive synchronization performance to go along with the greatest flexibility of any tiered code. Options 1 and 2 have the worst synchronization performance owing to the poor correlation performance of the short Gold codes used for their respective tertiary codes.

1.7 Q Channel Cross-Correlation Performance

The cross-correlation performance of each option was considered over a time difference of arrival (TDOA) of +/- 20 ms to account for a realistic cross-correlation scenario. This TDOA range is about two times the expected difference for between signals from GPS satellites and the results do not vary significantly for larger values of TDOA. The correlation results are computed over many possibilities to get adequate statistics. For example, in Option 5, the Monte Carlo analysis is run for 10230 offsets per primary chip, 20 instances of TDOA for primary chips between +/- 20 ms. This result also included 6000 starting points in increments of the primary code periods for the code being correlated, for each of 50 codes tracked and 49 codes interfering resulting in a total of 3,007,620,000,000 possibilities. Thus, a probability of occurrence of 3E-13 results if a value is only observed once.

The results provided with **Error! Reference source not found.** through **Error! Reference source not found.** have colors coded as follows:

- Red indicates a relatively poor cross-correlation value less than -32 dB
- Yellow indicates an acceptable value between -32 dB and -35 dB
- Green indicates a good cross-correlation value between -35 dB and -41 dB
- Blue indicates an exceptional cross-correlation values a less than -41 dB

Error! Reference source not found. through **Error! Reference source not found.** below assume that a receiver will exploit the pilot channel for tracking with a coherent integration of 100 ms or 200 ms and that acquisition can occur with a coherent integration time $T_i = 2\ ms$ (all options), $T_i = 8\ ms$ (Option 3) and $T_i = 20\ ms$ (Option 4), understanding that the acquisition complexity will scale with the product of the code period$\times T_i \times$Number of sidebands (=1 for BPSK signals and 2 for BOC). Thus, acquisition of the tiered primary×secondary code is not feasible with Options 1 and 2, and is 5 times the complexity of acquiring the L5 primary code for Option 4.

While Options 3 and 4 appear to have the worst performance during track based on the maximum cross-correlation described in **TABLE 7**, the probability of having this cross-correlation is less than one in 1E11 , with a 200 ms integration case (tracking). As an example, it is 71 thousand times more likely to win the California Super Lotto jackpot (odds of one in 42 million) than to have a max cross-correlation of -29.9 dB for the 200 ms case with Option 3. While several authors have used the max cross-correlation as a metric to compare the relative merits of different spreading and overlay codes [11] [24], the use of max cross-correlation is not a realistic figure of merit for

comparing the relative cross-correlation performance of different spreading code options and should only be used as a factor to select the best spreading codes within a family, as illustrated by **TABLE 7** and **TABLE 8** and. Readers should be careful to make practical decisions based on maximum cross-correlation results.

Instead, it is advisable to instead consider cross-correlation characteristics that describe some desired confidence level such as 99 % as described in **TABLE 9** or the rms values as described in **TABLE 10**. While Option 3 appears to be the worst option when considering the max cross-correlation for acquisition and tracking, it is amongst the best performers for tracking with 99 % confidence. In fact, when considering the 99th percentile results, all the options fare extraordinarily well during track with $T_i = 100\ ms$ or greater. In addition to low probability of having a cross-correlation event as the coherent integration is increased, longer coherent integrations offer additional protection through a correlator's response which scales as $\sin(\pi\Delta f_{ij}T_i)/(\pi\Delta f_{ij}T_i)$; where Δf_{ij} is the Doppler difference between the signal being acquired or tracked and the interfering signal. Considering that the AFS will be received by users with varying amounts of Doppler shift, the combined effect of cross-correlation and Doppler shift for a given integration time will further reduce these effects.

TABLE 7: Max cross-correlation for each option.

	PRN Sequesnce Length (chips)			Coherent Integration Period (ms)			99 % (Prob of Crosscorrelation < 1 %) (db)		
Option	Primary	Secondary	Tertiary	T_i Acq (ms)	T_i Track (ms)	Acq. 1,2 ms	Acq. 4, 8,20 ms	Track 100 ms	Track 200 ms
1	5115	100	120	1	100, 200	-24.2		-32.7	-32.9
2	10230	100	60	2	100, 200	-25.2		-32.6	-36.3
3	10230	4	1500	2,8	100, 200	-25.2	-27.0	-27.3	-29.9
4	10230	20	300	2,20	100, 200	-25.2	-27.2	-27.2	-27.2
5	10230	6000	N/A	2	100, 200	-25.2		-31.0	-32.9

TABLE 8: Probability of Max cross-correlation.

	PRN Sequesnce Length (chips)			Coherent Integration Period (ms)			Probability of Max Crosscorrelation		
Option	Primary	Secondary	Tertiary	T_i Acq (ms)	T_i Track (ms)	Acq. 1,2 ms	Acq. 4, 8,20 ms	Track 100 ms	Track 200 ms
1	5115	100	120	1	100, 200	3.1E-07		5.0E-12	2.3E-12
2	10230	100	60	2	100, 200	3.9E-08		1.0E-11	5.0E-12
3	10230	4	1500	2,8	100, 200	3.0E-08	1.2E-09	1.3E-12	3.3E-13
4	10230	20	300	2,20	100, 200	4.4E-08	2.0E-10	1.3E-12	7.0E-12
5	10230	6000	N/A	2	100, 200	4.0E-08		3.3E-13	6.7E-13

TABLE 9: 99 % Cross-Correlation for Each option.

	PRN Sequesnce Length (chips)			Coherent Integration Period (ms)			99 % (Prob of Cross-correlation < 1 %) (db)		
Option	Primary	Secondary	Tertiary	T_i Acq (ms)	T_i Track (ms)	Acq. 1,2 ms	Acq. 4,8,20 ms	Track 100 ms	Track 200 ms
1	5115	100	120	1	100, 200	-29.1		-46.8	-47.0
2	10230	100	60	2	100, 200	-31.7		-46.4	-49.4
3	10230	4	1500	2,8	100, 200	-31.7	-35.3	-45.2	-48.2
4	10230	20	300	2,20	100, 200	-31.7	-39.4	-45.4	-48.4
5	10230	6000	N/A	2	100, 200	-31.7		-46.4	-49.4

TABLE 10: RMS cross-correlation for each option.

	PRN Sequesnce Length (chips)			Coherent Integration Period (ms)			rms Cross-correlation (db)		
Option	Primary	Secondary	Tertiary	T_i Acq (ms)	T_i Track (ms)	Acq. 1,2 ms	Acq. 4, 8,20 ms	Track 100 ms	Track 200 ms
1	5115	100	120	1	100, 200	-37.1		-57.2	-57.4
2	10230	100	60	2	100, 200	-40.1		-57.1	-60.0
3	10230	4	1500	2,8	100, 200	-40.1	-46.1	-57.1	-60.1
4	10230	20	300	2,20	100, 200	-40.1	-50.0	-57.0	-60.0
5	10230	6000	N/A	2	100, 200	-40.1		-57.1	-60.1

Note that Option 3 has the best combination of good cross-correlation performance during acquisition and exceptional cross-correlation when tracking. It also provides exceptional performance at the rms average level. Observe that the cross-correlation generally scales with code period over which correlation occurs for the mean

and 99th percentile results. We find that the rms cross-correlation scales as expected with coherent integration and is a more conservative measure than the mean for initial comparisons as shown in **TABLE 10**.

1.8 Summary of AFS Pilot Signal Recommendations

As a result of the exceptional flexibility, excellent combination of cross-correlation performance under acquisition and tracking and excellent time to synchronize, Option 3 is recommended as the best Q channel signal option for the AFS signal specification. For this option, fifty 1500-symbol Weil sequences were created from a Weil code family. Primary sequences defined in the AFS specification should likely be chosen from L1C, L5 or a different code family with 210 or more spreading codes (like GPS).

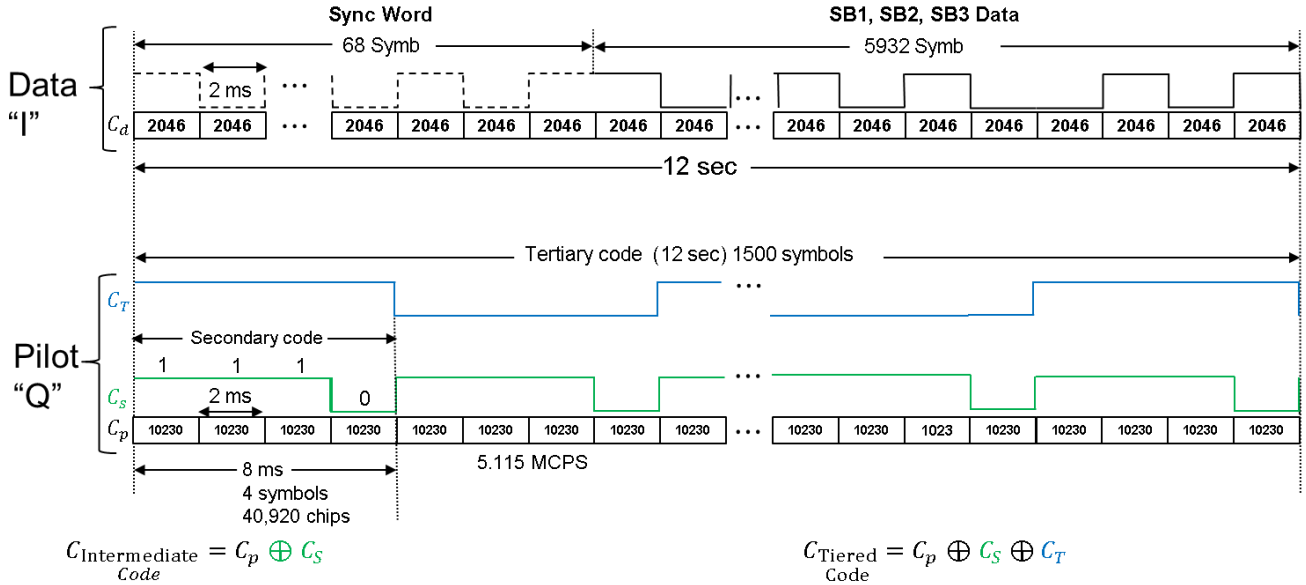

FIGURE 11: Recommended LunaNet data and pilot signal structure.

SUMMARY AND CONCLUSIONS

In conclusion, we have conducted an extensive trade study to recommend key aspects of the AFS signal structure including I and Q channel primary code lengths, synchronization word length, data modulation and frame structure, including 2-bit FID and 7-bit TOI specified within the 9-bit rate 9/52 BCH code in SB1. The results also describe the performance of the 5G NR FEC design recommended for use in the AFS and a 1.023 MCPS 2046-chip Gold code sequence in I channel.

A flexible pilot overlay structure was also described, which provides absolute time with a two or three step synchronization approach using a 10230-chip primary code, a 4-chip secondary code and 1500-chip tertiary code for the Q channel pilot at 5.115 MCPS. The overall design approach provides versatile capabilities for both low complexity and high-performance user receivers. The recommendations herein have been presented to stakeholders and are in consideration for the next revision of the LunaNet AFS specification.

1.9 Features Compared to Terrestrial GNSS Signals

The recommended AFS design considerations included in this paper, if implemented, offer the following features compared with terrestrial GNSS signals:

- The first I/Q signal that services two classes of users, providing capabilities comparable or better than GPS C/A code and L5 in one signal.

- Best cross-correlation performance of any 2046-chip code including BeiDou's B1B signal.

- The most flexible acquisition alternatives of any GNSS signal by enabling acquisition using a 2046-chip data channel primary code, with twice the complexity of GPS C/A code and immediate data symbol synchronization. One of two repeating pilot channel spreading codes can be acquired using a receiver with complexity comparable to L5-only primary code acquisition circuit with 6 dB better processing gain. This is achieved using a tiered 40920-chip (8 ms) pilot spreading code, along with the 10230 chip primary code. This approach also provides 6 dB lower rms cross-correlation than using the I channel primary spreading code alone, as is the case for L5 only receivers [23].

- The first use of commercial 5G standard in any MGNSS signal, permitting rapid encoder development and exploitation of commercial intellectual property.

- The best performing FEC of any GNSS signal, exceeding L1C's LDPC code E_b/N_0 threshold by 0.6 dB.

- The first use of a tertiary overlay code enabling flexible acquisition alternatives at higher processing gain.

- The first standalone data signal with a high integrity synchronization word to enable high reliability frame synchronization for decoding of BCH or LDPC encoded messages without a pilot channel overlay for reduced complexity Internet of things (IoT) receivers.

ACKNOWLEDGEMENTS

We would like to acknowledge the support of the National Aeronautics and Space Administration (NASA) under contract 80GSFC19D0011. This analysis was performed for NASA's Lunar Communications Relay and Navigation Systems (LCRNS) project to inform the LunaNet Interoperability Specifications. We especially acknowledge the feedback from NASA team leads Ms. Cheryl Gramling and Mr. Juan Crenshaw throughout the course of this work. Their insights were instrumental in establishing goals and milestones that led to a well thought-out and systematic trade of alternatives for the data and pilot channel recommendations described herein. The resulting analyses provide a firm set of reference performance characteristics, that provides traceability and rationale for the AFS specifications. We also acknowledge ongoing feedback from European Space Agency (ESA) and Japanese Space Exploration Agency (JAXA) representatives, which enabled us to recommend a solution that addresses stakeholders needs in the AFS development. Finally, we acknowledge ESA for the suggestion to incorporate a 2-bit FID into the BCH encoded SB1 together with a 7-bit TOI, and a 9-bit ITOW in SB2 of the navigation message. This approach provides increased flexibility, while accommodating the need for an I channel data frame synchronization word.

REFERENCES

[1] "LunaNet Position, Navigation, and Timing Services and Signal, Enabling the Future of Lunar Exploration," Pietro Giordano, Richard Swinden, Javier Ventura-Traveset, ESA. Cheryl Gramling and Juan Crenshaw, NASA.

[2] LunaNet Signal-In-Space Recommended Standard - Augmented Forward Signal (LSIS), Draft Version 5, August 31, 2023.

[3] "Description of the L1C Signal," John W. Betz, Mario A. Blanco, Charles R. Cahn, Philip A. Dafesh, Christopher J. Hegarty, Kenneth W. Hudnut, Vipada Kasemsri, Richard Keegan, Karl Kovach, Capt Lawrence S. Lenahan, Howard H. Ma, Joseph J. Rushanan, Dean Sklar, Thomas A. Stansell, Charles C. Wang, and Soon K. Yi.

[4] "Navistar GPS Space Segment/User Segment L1C Interface,"IS-GPS-800, 5 Sept 2012.

[5] P. A. Dafesh and J. K. Holmes, “Practical and Theoretical Tradeoffs of Active Parallel Correlator and Passive Matched Filter Acquisition Implementations,” Proceedings of the IAIN World Congress in association with the U.S. ION Annual Meeting, 26-28 June 2000, San Diego, CA.

[6] Philip Dafesh, “The GNSS Acquisition Time Enhancement (GATE) Signal,” Ion Pacific PNT conference, to be published.

[7] BeiDou Navigation Satellite System Signal in Space Interface Control Document, “Open Service Signal Version 2 .0., Dec. 2013.

[8] “Navistar GPS Space Segment Navigation User Interface,” ICD-GPS-200, IS-GPS-200H, 24 Sept, 2013.

[9] Sanjai Kohli, Steven Chen, Charle Cahn, Mangesh Chansarkar and Greg Teretsky, “Spread Spectrum Receiver with Multi-bit Correlator” U.S. Patent US 7,729,413 B2, filed April 2004.

[10] Sarwate, D.V., and M.B. Pursley. “Crosscorrelation Properties of Pseudorandom and Related Sequences.” *Proceedings of the IEEE,* Vol. 68, No. 5, May 1980, pp. 593–619.

[11] Joseph J. Rushannan, “The Spreading and Overlay Codes for the L1C Signal,” ION Journal of Navigation, Spring 2007.

[12] “Cramming More Components onto Integrated Circuits. Moors Law, https://www.intel.com/content/www/us/en/history/virtual-vault/articles/moores-law.html

[13] See https://www.u-blox.com/en/product/max-m10-series data sheet.

[14] European GNSS (GALILEO) Open Service Signal-In-Space Interface Control Document, Issue 2, Jan 2021. “Navistar GPS Space Segment/User Segment L5 Interface,” IS-GPS-800, 5 Sept 2012.

[15] RTCA DO-229F, “Minimum Operational Performance Standards (MOPS) for Global Positioning System /Satellite Based Augmentation System Airborne Equipment”, June 2020.

[16] Don Benson, “GPS L1 C/A Signal Acquisition Analysis,” September 21, 2006

[17] Sükrü Ekin Kocabas ¸and Abdullah Atalar, “Binary Sequences with Low Aperiodic Autocorrelation for Synchronization Purposes,” IEEE Communications Letters, vol.7, no.1, January 2003.

[18] “3GPP TS 38.212. Technical Specification Group Radio Access Network; NR; Multiplexing and channel coding (r18),” https://portal.3gpp.org/desktopmodules/specifications/SpecificationDetails.aspx?specificationId=3214

[19] Thorpe, Jeremy. "Low-density parity-check (LDPC) codes constructed from protographs." IPN progress report 42.154 (2003): 42-154.

[20] Hoydis, Jakob; et al. “Sionna: An Open-Source Library for Next-Generation Physical Layer Research.” March 2023. Available: https://arxiv.org/abs/2203.11854

[21] W. Ryan, “An Introduction to LDPC codes”, CRC Handbook for Coding and Signal Processing for Recording Systems, 2004.

[22] Galileo E6-B/C Codes Technical Note, Jan 2019.

[23] Tracy Cozzens, “OneNav unveils L5-only mobile GNSS receiver,” May 24, 2021

[24] Bradford Parkinson, et. al, “Gobal Positioning System: Theory and Applications,” First edition, pg105, 1996.

ACRONYMS

5GNR	5G new radio
AFS	Augmented Forward Signal
AWGN	Additive White Gaussian Noise
BCH	Bose–Chaudhuri–Hocquenghem
BOC	binary offset carrier
BPSK	binary phase-shift keying
C/A	Civilian Acquisition
CED	Clock and Ephemeris Data
FEC	Forward error correction
FFT	Fast Fourier Transform
FID	Frame identifier
GNSS	Global navigation satellite system
GPS	Global Positioning System
IP	Intellectual property
LANS	Lunar Augmented Navigation Service
LDPC	Low Density Parity Check
LLR	Log Likelihood Ratio
MCPS	Mega chips per second
NASA	National Aeronautics and Space Administration
Pd	Probability of detection
Pfa	Probability of false alarm
PNT	Position, Navigation and Timing
PRN	pseudo-random noise
rms	Root mean square
SB1, SB2, SB3, SB4	Subframes number 1, 2, 3 and 4
SWAP	Size, weight and power
TBC	to be confirmed

TBW	To be written
TOI	Time of Interval
TOW	Time of Week
TTFF	Time To First Fix